Atmospheric Environment 45 (2011) 223–234

Contents lists available at ScienceDirect

Atmospheric Environment

journal homepage: www.elsevier.com/locate/atmosenv

Modeling the fate of atmospheric reduced nitrogen during the Rocky Mountain Atmospheric Nitrogen and Sulfur Study (RoMANS): Performance evaluation and diagnosis using integrated processes rate analysis

Marco A. Rodriguez [a,*], Michael G. Barna [b], Kristi A. Gebhart [b], Jennifer L. Hand [a], Zachariah E. Adelman [c], Bret A. Schichtel [b], Jeffrey L. Collett Jr. [d], William C. Malm [a]

[a] Cooperative Institute for Research in the Atmosphere, Colorado State University, 1375-Campus Delivery, Fort Collins, CO 80523-1375, USA
[b] Air Resources Division, National Park Service, Fort Collins, CO 80523-1375, USA
[c] Institute for the Environment, University of North Carolina at Chapel Hill, Chapel Hill, NC 27599-6116, USA
[d] Department of Atmospheric Science, Colorado State University, Fort Collins, CO 80523, USA

ARTICLE INFO

Article history:
Received 21 May 2010
Received in revised form
18 August 2010
Accepted 3 September 2010

Keywords:
Ammonia
Reduced nitrogen
CAMx
Process analysis
RoMANS
Rocky Mountain National Park

ABSTRACT

Excess wet and dry deposition of nitrogen-containing compounds is a concern at a number of national parks. The Rocky Mountain Atmospheric Nitrogen and Sulfur Study (RoMANS) was conducted during the spring and summer of 2006 to identify the overall mix of ambient and deposited sulfur and nitrogen at Rocky Mountain National Park (RMNP), in north-central Colorado. The Comprehensive Air Quality Model with extensions (CAMx) was used to simulate the fate of gaseous and particulate species subjected to multiple chemical and physical processes during RoMANS. This study presents an operational evaluation with a special emphasis on the model performance of reduced nitrogen species. The evaluation showed large negative biases and errors at RMNP and the entire domain for ammonia; therefore the model was considered inadequate for future source apportionment applications. The CAMx Integrated Processes Rate (IPR) analysis tool was used to elucidate the potential causes behind the poor model performance. IPR served as a tool to diagnose the relative contributions of individual physical and chemical processes to the final concentrations of reduced nitrogen species. The IPR analysis revealed that dry deposition is the largest sink of ammonia in the model, with some cells losing almost 100% of the available mass. Closer examination of the ammonia dry deposition velocities in CAMx found that they were up to a factor of 10 larger than those reported in the literature. A series of sensitivity simulations were then performed by changing the original deposition velocities with a simple multiplicative scaling factor. These simulations showed that even when the dry deposition values were altered to reduce their influence, the model was still unable to replicate the observed time series; i.e., it fixed the average bias, but it did not improve the precision.

1. Introduction

Excess wet and dry deposition of nitrogen-containing compounds, such as nitric acid (HNO_3), particulate ammonium (NH_4^+), particulate nitrate (NO_3^-), and ammonia (NH_3), is a concern at a number of national parks. Rocky Mountain National Park (RMNP), in north-central Colorado, provides a well-documented example of the role of excess nitrogen deposition in sensitive alpine environments and its potential to influence ecosystem dynamics (Baron, 2006; Baron et al., 2000; Korb and Ranker, 2001; Nydick et al., 2004). Human activity, including combustion of fossil fuels, application of nitrogen fertilizers, confined animal feedlot operations (CAFO), and cultivation of nitrogen-fixing legumes, has substantially altered the global nitrogen cycle (Galloway et al., 2003). Wet and dry deposition of reduced nitrogen ($N(-III) = NH_3 + NH_4^+$) and atmospheric oxidation products of nitrogen oxides ($NO_x = NO + NO_2$) are significant nitrogen inputs in many environments.

To investigate nitrogen deposition at RMNP, and to elucidate the nitrogen sources that are impacting the park, the National Park Service initiated the Rocky Mountain Atmospheric Nitrogen and Sulfur Study (RoMANS) (Beem et al., 2010; Malm et al., 2009; Levin et al., 2009). The RoMANS study included two 5-week sampling periods in 2006. The first was a spring campaign from March 23

* Corresponding author. Tel.: +1 970 491 8101; fax: +1 970 491 8598.
E-mail address: rodriguez@cira.colostate.edu (M.A. Rodriguez).

1352-2310/$ – see front matter © 2010 Elsevier Ltd. All rights reserved.
doi:10.1016/j.atmosenv.2010.09.011

through April 30 and the second a summer campaign from July 6 through August 12. Upslope easterly flow that can bring emissions from the east (the Front Range region – which includes the Denver metropolitan area – and beyond) is more common during hours of precipitation than during non-precipitating hours for all seasons. However, climatologically, wet deposition during spring and summer is associated with precipitation from different types of meteorological regimes. Spring precipitation is mostly due to large-scale storms associated with widespread regional precipitation, while summer precipitation is mostly due to small-scale afternoon convective activity due to air masses rising over the mountains. The frequency of easterly flow when precipitation also occurs is greater during spring than summer, but the vertical depth of easterly flow is often greater during summer than spring.

CAMx (Comprehensive Air Quality Model with extensions version 4.51; ENVIRON, 2005), an advanced eulerian chemical transport model (CTM), was used to simulate the ambient concentrations of nitrogen and sulfur species during the two RoMANS sampling periods. Although CAMx has been used extensively to simulate regional sulfate and ozone (Yarwood et al., 2003; Morris et al., 2004), and to a lesser degree nitrate and nitric acid (Baker and Scheff, 2007), its application to modeling ammonia and organic nitrogen in regions of complex terrain has been limited. As part of RoMANS, the National Park Service had great interest in conducting the current modeling effort with the original intent to provide greater insight into the source types and regions that contribute the most to nitrogen deposition, especially NH_3, at RMNP. The source apportionment analysis can be reliable only if a performance evaluation of the regional modeling system properly assesses the suitability of the model to this type of application (Barna et al., 2006; Jiménez et al., 2006; Morris et al., 2006; Pun et al., 2006; Tesche et al., 2006; Tonnesen et al., 2006). The first part of this study provides an operational model evaluation with special emphasis on the model performance of reduced nitrogen species. This evaluation relies on the RoMANS dataset, which is unique in that it provides high time resolution measurements of NH_3, a species not routinely measured, at the core site located in RMNP. Realizing that the model performance for reduced nitrogen, but especially NH_3, leaves the model unsuitable for source apportionment applications, the second part of this work concentrates on a model diagnosis to investigate the underlying causes of this poor performance. The CAMx 'integrated processes rate analysis' tool was used for an in-depth analysis of the model performance and to reveal the relative contributions from individual physical and chemical processes (e.g., emissions, chemistry, deposition, and transport) to the predicted concentrations of nitrogen species. Finally, guided by the process analysis results, the effects of different deposition velocities on the predicted NH_3 concentrations were investigated through a series of sensitivity simulations where a simple multiplicative factor modifies the original deposition velocities values.

2. Modeling system description

The air quality modeling system consisted of three major components: CAMx, a CTM; the Penn State University/NCAR Mesoscale Model (known as MM5), a regional weather model (Grell et al., 1994); and SMOKE (Sparse Matrix Operator Kernel Emissions; Houyoux et al., 2002; IE, 2006), an emissions processing system that transforms emissions inventory data to the chemical, spatial, and temporal terms required by the CTM. CAMx was run with two-way grid nesting, using three domains with horizontal grid size resolutions of 36 km, 12 km, and 4 km (Fig. 1). The 36-km outer domain covered the contiguous United States, southern Canada, and northern Mexico. The 4-km inner domain extends over most of Colorado, and the 12-km domain encompassed the surrounding states. The horizontal model domains were specified using an 'Arakawa C' grid, and sigma pressure levels were used in the vertical dimension.

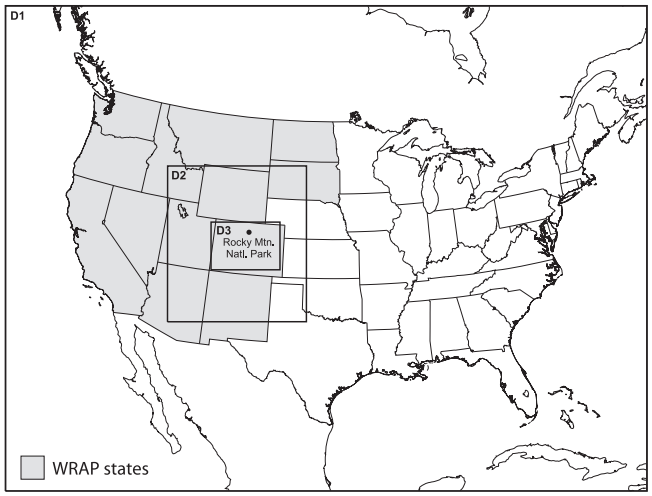

Fig. 1. Map of the three nested computational domains used in this study. The outer domain (D1) covers the contiguous United States, northern Mexico and southern Canada with a horizontal grid resolution of 36 km. The inner domain (D3) extends over most of Colorado with a grid resolution of 4 km, while D2 encompasses the surrounding states with a grid resolution of 12 km. The states in gray are part of the Western Regional Air Partnership (WRAP) regional planning organization.

Horizontal advection was treated with the piecewise-parabolic method (PPM), an area-preserving, flux-form advection solver with explicit horizontal diffusion (Odman and Ingram, 1996). Gas-phase chemistry was based on the Carbon Bond IV mechanism (Whitten et al., 1996). ISORROPIA (version 1.6), a thermodynamic equilibrium model (Nenes et al., 1999), was used to predict the partitioning of inorganic aerosol constituents (sulfate, nitrate, and ammonium) between the gas and particle phases. CAMx represents aerosol size distributions with a sectional approach, and in particular this study used the CF scheme that divides the size distribution into two static modes (coarse and fine). The CAMx outputs include hourly average concentrations for gas and particulate species. MM5 provided the wind fields that CAMx needed to determine the transport of chemical species, as well as other meteorological variables such as temperature, pressure, and precipitation.

The SMOKE processing system was used to prepare the emissions inventory data in a prescribed format that reflected the spatial, temporal, and chemical speciation parameters required by CAMx on the RoMANS nested domains (Fig. 1). Developing an approach to estimate air pollutant emissions that were representative of the RoMANS field study period was necessary since 2006 inventory data were not readily available for North America at the time this study took place. For most of the emissions sectors, such as on-road mobile and stationary area sources, inventories developed by the U.S. Regional Planning Organizations (RPOs) to support regional haze state implementation plan (SIP) modeling were used (Morris et al., 2007; Pechan, 2003). In particular, the inventories and methodologies developed by the Western Regional Air Partnership (WRAP) were employed as a starting point for developing the RoMANS inventory (Tonnesen et al., 2006). The emissions database was built using the WRAP inventory developed for 2002 and that consists of 22 different categories (e.g., automobiles, power plants, forest fires, oil and gas development, etc.). Given the potentially large contribution of NH_3 to overall nitrogen deposition at RMNP, the WRAP NH_3 emissions inventory was updated in an attempt to capture the local and regional NH_3 emissions patterns

more accurately. Additionally, the point biogenic, and mobile sources were updated to reflect 2006 emissions.

Emissions from agriculture and CAFO activities were the primary sources of NH_3. The present NH_3 emission inventory model uses a geographic information system to couple land-use data with emissions factors and gridded meteorology data to calculate hourly NH_3 emissions within the United States (Mansell, 2005). The model calculated NH_3 emissions from fertilizer, livestock, domestic animals, wild animals, and soil. All of these NH_3 emissions processes were estimated for the WRAP states in the three RoMANS modeling grids during the study periods, with the exception of soil NH_3 due to uncertainties in the emissions factors for this process. The fertilizer sector used monthly emissions factors; the rest of the other sectors used annual emissions factors. County-level NH_3 emissions estimates contained in the stationary area inventories were used for the rest of the modeling domain. Tables S1 and S2 in the Supplementary Materials section summarize gridded U.S. and Colorado-only total annual emissions by major emissions source categories.

3. Model performance evaluation

The focus of this evaluation was aerosol and gaseous species pertinent to RoMANS. Seigneur et al. (2000) presented several standard performance metrics commonly applied to the evaluation of air quality models. This study favors the use of the mean fractional error (MFE) and the mean fractional bias (MFB) as defined by Boylan and Russell (2006). One key advantage to using MFB and MFE is that by normalizing the concentration difference with the sum of the observed and predicted concentrations, as opposed to normalizing with the observed concentration alone, the MFE and MFB are restricted from growing too large when very small observed concentrations are considered. Additionally, the metrics that define the MFB and MFE bound the maximum and minimum bias and error and do not allow a few data points to dominate the calculated bias and error; also, the metrics are symmetric because they give equal weight, on a relative basis, to concentrations simulated higher as well as those simulated lower than observations. The discussion on the model performance in the following sections is based mostly on the MFE and MFB. However, the tables that summarize these values show additional statistics like the mean bias and mean error that appear in other model evaluations and are provided to allow the readers a comparison of this study's results to a larger range of model evaluations.

3.1. Model performance evaluation using IMPROVE data for the United States

A coarse-scale evaluation of simulated particulate sulfate and nitrate was performed with results from the 36-km CAMx domain and available speciated fine particulate concentrations (<2.5 micrometers in diameter) collected from the Interagency Monitoring of Protected Visual Environments (IMPROVE) monitoring network (Malm et al., 1994; DeBell et al., 2006). The IMPROVE network collects 24 h average samples every third day.

Table 1 summarizes the model performance statistics for both the entire 36-km domain and the sites that fall within the western United States as determined by the WRAP region (Fig. 1). Results show that the model underestimated observed sulfate concentrations both in spring and summer, but the negative biases were higher during the summer. The calculated MFE for sulfate showed that the model deviates from observations even more during the summer than spring by an additional 5% on average. In this study, the MFB in the western states during spring was -23%. For comparison, the MFB in the WRAP-RMC (Regional Modeling Center) simulations for 2002 was approximately −40% (Tonnesen et al., 2006). During summer the estimated MFB was −46%, while in the WRAP-RMC it was close to −20%.

The model also underestimated the nitrate concentrations both in spring and summer, with larger negative biases during the summer. The equilibrium dissociation constant for ammonium nitrate is quite sensitive to temperature changes, varying over more than two orders of magnitude for typical ambient conditions. In general, lower temperatures shift the equilibrium system toward the aerosol phase. Hence, a possible explanation for the observed seasonal biases of nitrate is that at colder temperatures, particle

Table 1
Model performance statistics for particulate sulfate and particulate nitrate concentrations during both the 2006 spring and summer RoMANS field campaigns, using available IMPROVE monitoring stations for the entire U.S. domain and sites that fall within the western United States alone. Comparison is made with model simulation values from the 36-km domain.

	Spring				Summer			
	U.S.		West		U.S.		West	
	SO_4^{2-} ($\mu g\,m^{-3}$)	NO_3^- ($\mu g\,m^{-3}$)	SO_4^{2-} ($\mu g\,m^{-3}$)	NO_3^- ($\mu g\,m^{-3}$)	SO_4^{2-} ($\mu g\,m^{-3}$)	NO_3^- ($\mu g\,m^{-3}$)	SO_4^{2-} ($\mu g\,m^{-3}$)	NO_3^- ($\mu g\,m^{-3}$)
Mean obs.	1.50	0.45	0.67	0.27	2.47	0.21	1.01	0.19
Mean sim	1.77	0.67	0.54	0.47	1.85	0.10	0.64	0.10
Number[a]	1427	1437	797	816	1438	1444	829	841
STD[b] obs.	1.6	0.7	0.5	0.5	2.7	0.3	0.7	0.3
STD sim	2.3	1.0	0.5	0.8	2.9	0.3	0.6	0.4
r[c]	0.76	0.50	0.48	0.37	0.75	0.11	0.48	0.40
MB[d]	0.3	0.2	−0.1	0.2	−0.6	−0.1	−0.4	−0.1
MNB[e] (%)	30%	261%	8%	344%	−16%	−26%	−21%	−14%
ME[f]	0.9	0.6	0.4	0.4	1.2	0.2	0.5	0.2
MNE[g] (%)	75%	337%	65%	416%	57%	127%	57%	137%
MFE[h] (%)	57%	119%	58%	118%	62%	160%	63%	160%
MFB[i] (%)	−6%	−17%	−23%	−9%	−42%	−133%	−46%	−129%

[a] Number of data pairs.
[b] Standard Deviation.
[c] Pearson's correlation coefficient.
[d] Mean Bias.
[e] Mean Normalized Bias.
[f] Mean Error.
[g] Mean Normalized Error.
[h] Mean Fractional Error.
[i] Mean Fractional Bias.

nitrate formation is favored, while at warmer temperatures it dissociates, leaving more available NH_3 in the gas phase, in turn resulting in a greater dependence during the summer than winter to the model NH_3 emissions and deposition magnitudes. The MFB in the western states during spring was −9%, while the WRAP-RMC 2002 MFB was approximately −50%. For July 2006 the estimated MFB was −129%, while the 2002 WRAP-RMC value was approximately −150% (Tonnesen et al., 2006). The estimated MFE showed that the model errors varied between 120% in the spring to 160% in the summer. These results show that the model errors for nitrate were far larger than those for sulfate concentrations, consistent with the WRAP-RMC results.

3.2. Model performance evaluation at the RoMANS satellite sites

The most extensive measurements during the RoMANS field study with the highest time resolution (hourly) were made at the core site in RMNP. Measurements at secondary sites (Lyons and Gore Pass, Colorado) were somewhat more sophisticated in terms of measurement capabilities than the remaining "satellite" sites in the study (Fig. 2). Beem et al. (2010) provided a complete listing of site names, locations, and operating periods for the measurements, while Levin et al. (2009) and Malm et al. (2009) provided a complete description of the measurement technology used during the RoMANS field study. An evaluation of measured and simulated aerosol and gas concentrations was performed at the available satellite sites for both spring and summer.

In addition to particulate sulfate and nitrate, other measured species in both the gas and aerosol phases (NH_3, HNO_3, SO_2, and NH_4^+) were compared with model results. Seasonal means and performance statistics were computed at each of the sites for each season. For all the satellite sites the comparison was made with model data from the 4-km domain. The only exception was Grant, Nebraska, that falls outside the 4-km domain and therefore 12-km domain data were used instead.

The mean predicted and observed concentrations for all particulate and gas-phase nitrogen and sulfur species as a function of site location during the spring and summer campaigns are shown in Fig. 2a and b, respectively. These figures provide an overview of the level of agreement between model and observations. In general, the largest measured and modeled concentrations for most species occurred in eastern Colorado. However, there were significant differences at many sites. For instance, during both the spring and summer, the model underestimated NH_3 concentrations by a factor of 3 at Brush, located in eastern Colorado, while SO_2 concentrations were overestimated by a factor of 5. Furthermore, the model underestimated NH_3 and NH_4^+ concentrations for all sites in both seasons. Modeled NO_3^- concentrations were low, but on the same order of magnitude of observations, with the exception of some RMNP sites with underestimations of up to one order of magnitude. HNO_3 and SO_4^{2-} were the only species that consistently had comparable concentrations between model and observations.

Figs. S1 to S6 in the Supplementary Materials section provide spring and summer 24-h average time series comparisons between model and observations that illustrate three selected RoMANS sites: Gore Pass, Colorado, located west of the Continental Divide (Figs. S1 and S2), Beaver Meadows in RMNP (Figs. S3 and S4) and Brush, Colorado, (Figs. S5 and S6) located east of the Continental Divide. These comparisons have the added advantage of higher time resolution. Measurements at Beaver Meadows illustrate the impacts of easterly transport east of the Continental Divide, where the events of April 20 and April 23 increase the concentrations of NH_3, particulates (NH_4^+, NO_3^-, SO_4^{2-}), and to a lesser extent HNO_3. During this same period, west of the Continental Divide at Gore Pass the concentrations are subjected to westerly flow and seem more uniform with less distinct episodes. The model, especially for the spring, has a very difficult time reproducing the observed daily concentrations. Across these sites and for both seasons the simulated NH_3 concentrations consistently underpredicted observations. The largest underestimation occurred at Brush where modeled NH_3 was a factor of 10 lower than observations. This site is located near CAFO operations and therefore closer to emission sources. However, for SO_4^{2-} the model is able to reproduce on average the observed concentrations. It is also evident from these figures that the model overestimates SO_2 for all sites and seasons.

3.3. Model performance evaluation for high time resolution observations at Rocky Mountain National Park

The core site located at RMNP was the only location where hourly observations were collected during RoMANS. The

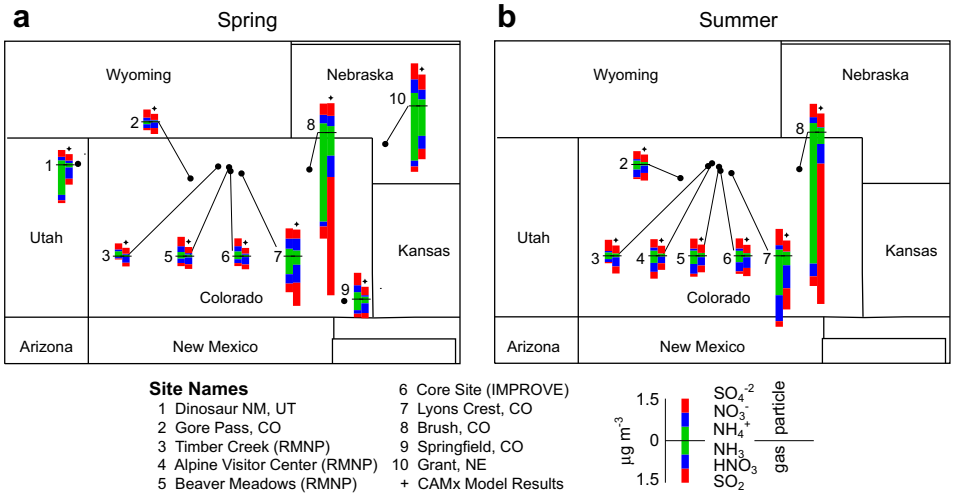

Fig. 2. Mean predicted and observed 24-h average particulate and gas-phase species concentrations (μg m^{-3}) for (a) spring and (b) summer. Particulate species are shown as the upper bar charts and gas-phase species are shown as the lower bar charts (see legend for scale). The predicted concentrations are shown with a "+" over the bar chart. Site locations correspond to the numbers listed next to the bar chart. The number of data pairs varied by season, species and site, but generally the means were calculated with 30 to 35 data pairs per site.

performance evaluation statistics for hourly concentrations of NH_3, NH_4^+, NO_3^-, SO_4^{2-}, SO_2, NO_x, and O_3 are presented in Table 2.

In general, the model underpredicted observed concentrations for particulate NO_3^- during both seasons, although both the biases and errors are smaller for spring than summer. Again, this could be due to particle nitrate formation favored at colder temperatures, thus decreasing the biases in spring. Nitric acid hourly concentrations were not available at the core site; however, a comparison between model oxidized nitrogen ($N(V) = HNO_3 + NO_3^-$) and particle NO_3^- was performed (not shown in Table 2). In general the comparison between model N(V) and particulate NO_3^- led to small, positive biases and reduced errors. This implied that to some extent the thermodynamical model had some difficulty in partitioning nitric acid between the gas and aerosol phases.

For reduced nitrogen ($N(-III) = NH_3 + NH_4^+$) species, the errors in the NH_4^+ and NH_3 predictions were 111% and 83%, respectively, during the spring. During the summer months, the errors in the NH_4^+ and NH_3 predictions were 70% and 135%, respectively. Estimates of the biases were negative for all species and both seasons, indicating a systematic model underestimation for these species. During spring, NH_3 had the lowest MFB (−38%) and NH_4^+ had the highest (−95%), compared to summer when NH_4^+ MFB was lowest (−61%) and NH_3 was highest (−131%).

Time series comparisons between reduced nitrogen model concentrations and observations using hourly values from the core site are shown in Figs. 3 (spring) and 4 (summer). In the spring, the measured NH_3 concentrations were low on average ($\sim 0.1\ \mu g\ m^{-3}$) except for two distinct episodes on April 20 and April 23 when the NH_3 observations were as high as $0.7\ \mu g\ m^{-3}$and NH_4^+ concentrations were close to $2\ \mu g\ m^{-3}$. Beem et al. (2010) and Malm et al. (2009) found that these periods of higher concentrations were commonly observed in both spring and summer during periods when upslope transport brought air from the east into RMNP. This is not surprising given the large emissions found in the nearby population centers along the Front Range urban corridor, which includes Denver, and agricultural regions east of the Rockies. In general, the model underestimated both NH_3 and NH_4^+ in the spring, with the exception of a few days (April 4, 8, and 13) when the model overestimated NH_3 observations. NH_4^+ values are always underestimated by the model regardless of the season. The model also tended to have difficulty simulating the timing of high-concentration events, with particular problems simulating the two events identified above. In fact, during the high observed NH_3 event on April 23, the predicted NH_3 was the lowest for the entire spring campaign. For NH_4^+ also the model seems to have difficulty in correctly predicting the timing of these upslope events.

During summer, two main episodes occur for NH_3: one during July 23 (peak of $\sim 2.9\ \mu g\ m^{-3}$) and a second during August 8 (peak of $\sim 1.8\ \mu g\ m^{-3}$). For measured NH_4^+ the peaks occur during July 22 (peak of $\sim 1\ \mu g\ m^{-3}$) and July 29 (peak of $\sim 1.5\ \mu g\ m^{-3}$). The second peak in NH_4^+ does not coincide in time with that of NH_3, indicating possible impacts from particulates (ammonium, sulfate, nitrate) more than from NH_3 transport alone. During summer the model showed a systematic negative bias for NH_3, but the timing seemed better relative to the spring results. The observations showed a marked diurnal variation that the model also seemed to

Table 2
Model performance statistics during both 2006 spring and summer RoMANS field campaigns. Hourly ambient data from the core site at Rocky Mountain National Park are compared with model simulation values from the 4-km domain.

	Spring						
	O_3 (ppb)	NO_x (ppb)	NO_3^- ($\mu g\ m^{-3}$)	NH_3 ($\mu g\ m^{-3}$)	NH_4^+ ($\mu g\ m^{-3}$)	SO_4^{2-} ($\mu g\ m^{-3}$)	SO_2 ($\mu g\ m^{-3}$)
Mean obs.	49.9	1.7	0.48	0.10	0.38	0.53	0.14
Mean sim	60.4	0.6	0.11	0.07	0.10	0.35	0.28
Number[a]	724	639	343	617	521	728	719
STD[b] obs.	9.5	1.2	0.67	0.10	0.31	0.37	0.20
STD sim	9.9	0.6	0.25	0.07	0.10	0.25	0.48
r[c]	0.29	0.39	0.15	0.10	0.28	0.18	0.08
MB[d]	10.5	−1.1	−0.4	−0.03	−0.3	−0.2	0.1
MNB[e] (%)	25%	−59%	−50%	47%	−40%	11%	10292%
ME[f]	12.2	1.2	0.4	0.07	0.3	0.4	0.2
MNE[g] (%)	28%	64%	105%	125%	84%	87%	10325%
MFE[h](%)	23%	100%	156%	83%	111%	77%	103%
MFB[i](%)	19%	−96%	−138%	−38%	−95%	−35%	53%
	Summer						
	O_3 (ppb)	NO_x (ppb)	NO_3^- ($\mu g\ m^{-3}$)	NH_3 ($\mu g\ m^{-3}$)	NH_4^+ ($\mu g\ m^{-3}$)	SO_4^{2-} ($\mu g\ m^{-3}$)	SO_2 ($\mu g\ m^{-3}$)
Mean obs.	46.8	1.9	0.18	0.43	0.34	0.66	0.16
Mean sim	41.5	0.7	0.01	0.09	0.17	0.53	0.53
Number[a]	788	724	727	731	727	727	778
STD[b] obs.	13.9	0.9	0.29	0.32	0.21	0.23	0.17
STD sim	9.7	0.8	0.07	0.13	0.09	0.32	0.75
r[c]	0.49	0.27	0.03	0.15	0.21	0.13	0.23
MB[d]	−5.3	−1.2	−0.2	−0.33	−0.2	−0.1	0.4
MNB[e] (%)	−5%	−62%	−90%	−73%	−39%	−11%	459%
ME[f]	10.9	1.3	0.2	0.4	0.2	0.3	0.4
MNE[g] (%)	25%	69%	100%	79%	51%	46%	469%
MFE[h](%)	25%	108%	189%	135%	70%	50%	102%
MFB[i](%)	−10%	−104%	−186%	−131%	−61%	−28%	88%

[a] Number of data pairs.
[b] Standard Deviation.
[c] Pearson's correlation coefficient.
[d] Mean Bias.
[e] Mean Normalized Bias.
[f] Mean Error.
[g] Mean Normalized Error.
[h] Mean Fractional Error.
[i] Mean Fractional Bias.

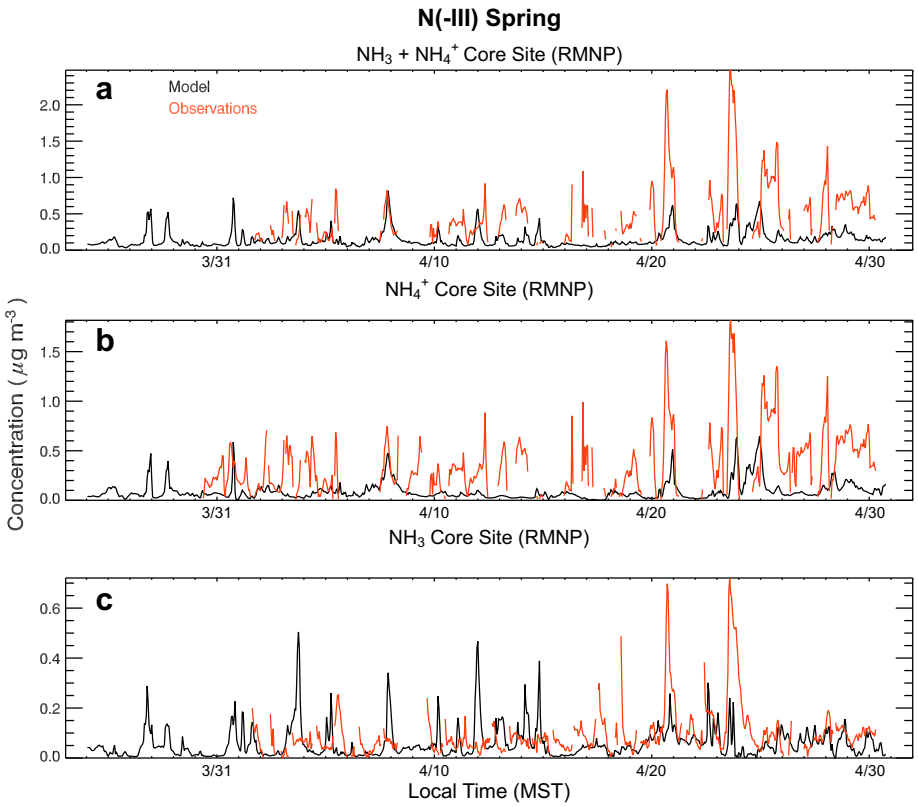

Fig. 3. Time series comparison at the core site located in Rocky Mountain National Park (RMNP) during the spring campaign (March 23 to April 30, 2006) between hourly model results (in black) and observed ambient concentrations (in red) of (a) reduced nitrogen ($N(-III) = NH_4^+(p) + NH_3(g)$), (b) NH_4^+, and (c) NH_3. Some observed values at the beginning of each period were not considered valid and neglected accordingly. The model results presented at the beginning of each period are not for spin up days. Units of $\mu g\,m^{-3}$ (For interpretation of the references to color in this figure legend, the reader is referred to the web version of this article.).

reproduce. Although model NH_4^+ during the summer is not able to correctly reproduce the timing of peak events, in general the average values are closer to observations than during spring.

In summary, the evaluation showed that the model exhibits poor performance for reduced nitrogen species during both RoMANS periods. There were not only large negative biases and errors at RMNP but also throughout the entire domain; therefore the model was deemed inadequate for any subsequent source apportionment applications. It was this inability of the model to capture important NH_3 episodes that motivated the application of process analysis, with the aim of diagnosing which mechanisms within the model were most relevant to simulating ambient ammonia concentrations.

4. Model diagnosis using integrated processes rate analysis

Process analysis (PA) has been incorporated into current air quality models, including CAMx, to examine model predictions in more detail. PA tracks the physical and chemical processes that affect concentrations estimated by the model, including advective and diffusive transport, gas and particle chemistry, emissions, and wet and dry deposition (Jeffries and Tonnesen, 1994). PA has been used extensively in regional air quality models to understand the processes involved in ozone formation (Henderson et al., 2010; Song et al., 2008; Vizuete et al., 2008; Kimura et al., 2008; Zhang et al., 2006). In this work, the information PA provided was used to understand the poor model performance of NH_3 concentrations.

Integrated Processes Rate (IPR) analysis (ENVIRON, 2005) was used, as this yields the most detail regarding the processes in the model. IPR provided detailed process rate information in the form of mass fluxes for each physical and chemical process for selected grid cells and selected species (Wang et al., 1995). Fig. 5 shows the mass fluxes corresponding to the individual processes that contributed to the concentration of ammonia during spring and summer for the 4-km grid cell that contained the RoMANS core site at RMNP. This figure illustrates that the most important gains (positive mass flux) at the site were the horizontal transport (both horizontal advection and diffusion) and the local emissions, while the major losses were vertical transport and dry deposition. The inorganic chemistry contribution, i.e. thermodynamic phase partitioning, was relatively small compared to other processes. At the core site during precipitation events, the relative humidity was high, thus favoring the formation of NH_4^+ from available NH_3, which was instantly removed by wet deposition in the model. The NH_3 that was lost through wet deposition is first lost into NH_4^+ through inorganic chemistry and then removed by NH_4^+ wet deposition. The model's performance to estimate wet deposition correctly at any given site depends in part on the driving meteorological model's ability to produce the correct spatial pattern and amount of precipitation. The RoMANS report (Malm et al., 2009) presents a quality assurance evaluation of the RoMANS MM5 data, and one of its findings was that MM5 did well in predicting where and when rain occurred, but generally overpredicted rainfall quantities; also there was better agreement during the cooler months than in the summer when convection dominates. During the spring, the inorganic chemistry mostly led to losses of NH_3 at RMNP, but there were a few instances in which it led to gains. In contrast, during the summer the inorganic chemistry was a net loss of NH_3.

To compare the relative magnitude of the fluxes from each process across a larger spatial domain, the IPR results for the

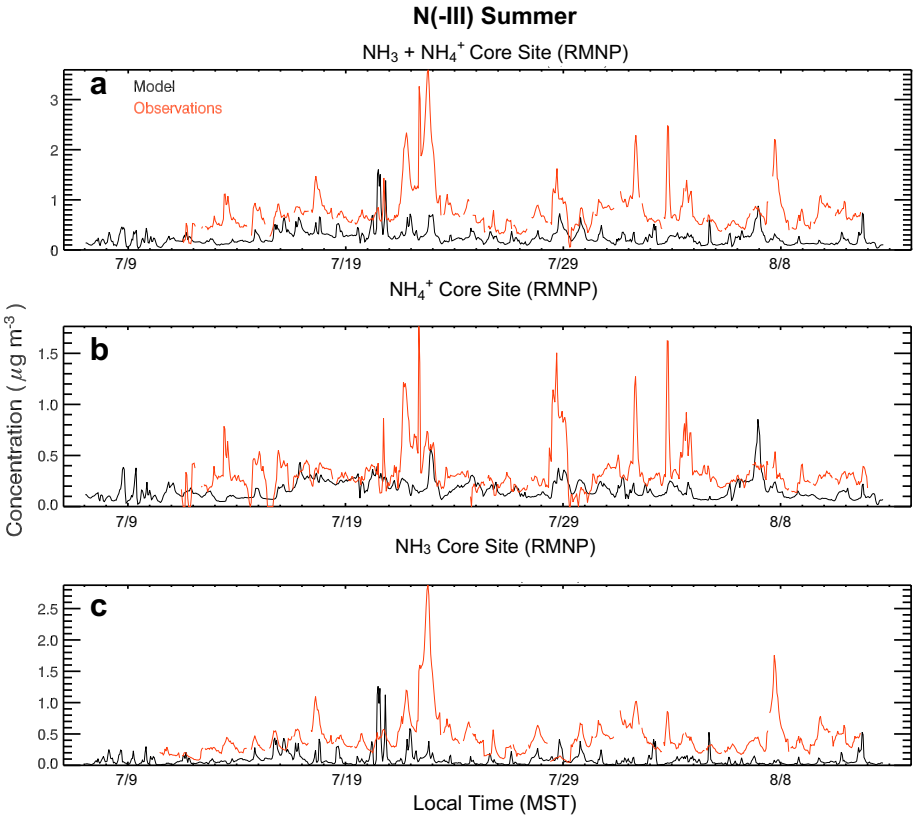

Fig. 4. Time series comparison at the core site located in Rocky Mountain National Park (RMNP) during the summer campaign (July 6 to August 12, 2006) between hourly model results (in black) and observed ambient concentrations (in red) of (a) reduced nitrogen (N(-III) = $NH_4^+(p) + NH_3(g)$), (b) NH_4^+, and (c) NH_3. Some observed values at the beginning of each period were not considered valid and neglected accordingly. The model results presented at the beginning of each period are not for spin up days. Units of $\mu g\,m^{-3}$ (For interpretation of the references to color in this figure legend, the reader is referred to the web version of this article.).

surface layer of each cell were added over the spring period and presented as isopleths in Fig. 6. This figure shows that emissions were the most important source of ammonia at the surface, while the NH_3 dry deposition acted as an important sink whose spatial distribution correlated strongly with the emissions spatial pattern. Fig. 6 also shows that vertical diffusion was the second largest loss of surface-level NH_3, and its spatial distribution correlated with the emissions. The aerosol chemistry acted as both a gain and a loss of NH_3, depending on the region, but for most of Colorado it was either a weak loss or had a negligible contribution to the mass flux. In order to have a first-order estimate of how strong was the removal of NH_3 due to dry deposition, the following estimate of the fraction of mass loss through dry deposition F_{DD} relative to the total available mass was performed for each cell of the 36-km cell domain (Fig. 7),

$$F_{DD} = \frac{DD}{C_0 + \sum_{i=1}^{N} P_i} \quad (1)$$

where C_0 is the initial mass in a given cell, P_i is the net positive flux into the cell due to each of the processes i, and DD is the mass loss through dry deposition alone. Fig. 7 shows that dry deposition removed as much as 30–40% of the available mass in the region that included RMNP. In some places, like the Pacific Northwest, the removal was larger, approaching almost 100% of the available mass. For most of the eastern United States, the losses ranged between 40% and 60%, and in many of the regions identified as important sources of NH_3 (the Midwest), the losses were as high as 50%.

In general, the NH_3 dry deposition losses accounted for about 50% of the total mass lost, but at particular times and locations it was as large as 100%. The second most important loss of NH_3 was vertical transport (on average 43% of the total loss), while the inorganic aerosol chemistry accounted for only 6% of the total loss. Although an important loss during the NH_3 episode observed at the core site on April 23, dry deposition only accounted for 20–30% of the total NH_3 loss, while about 50–60% of the loss was due to the vertical transport, and 20–30% was due to chemical transformation into NH_4^+.

The PA indicated that on average dry deposition was the process that led to the largest losses of NH_3 in the model and this could explain the systematic underestimation of NH_3 demonstrated in previous sections. However, given the uncertainties in the emissions inventories, and despite the updates detailed above, it is also possible that the net fluxes of NH_3 might be underestimated or that the location and timing of these fluxes were misrepresented, which could also lead to a negative bias. It was beyond the scope of the current study to evaluate the current NH_3 emissions inventory, and with the losses due to dry deposition in some model grid cells approaching 100% of the available NH_3 mass, it seemed reasonable to examine the causes behind the possible model overestimation of NH_3 dry deposition.

5. Sensitivity simulations with different deposition velocities

A starting point to investigate the overestimation of NH_3 dry deposition was to inspect the deposition velocity implementation in CAMx. NH_3 dry deposition velocities (v_d) are difficult to estimate and there is wide range of values reported in the literature (Andersen et al., 1993; Andersen and Hovmand 1995, 1999;

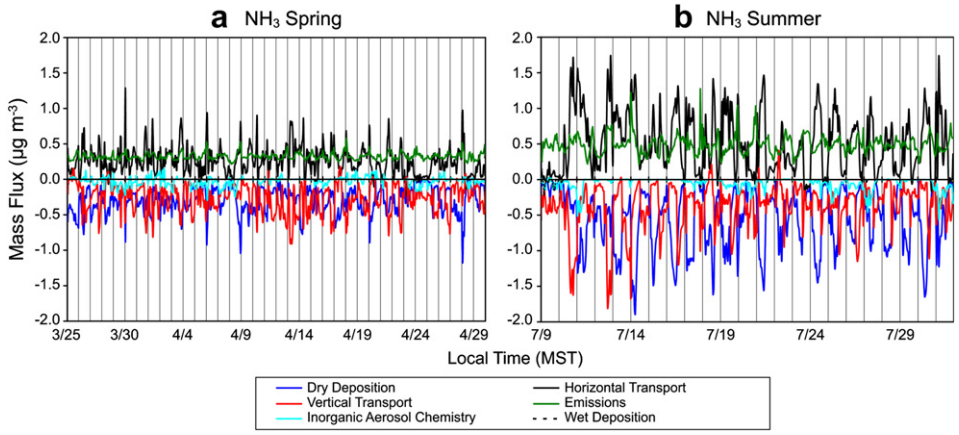

Fig. 5. Contribution of individual processes to the concentration of ammonia during (a) spring and (b) summer 2006 for the 4 km grid cell that contains the core site at Rocky Mountain National Park. Positive values indicate mass being added to the grid volume, negative values indicate mass being removed.

Andersen et al., 1999; Harrison and Allen, 1991; Zimmerling et al., 1997) with values as low as 0.3 cm s^{-1} (Nemitz et al., 2004) and as high as 4.6 cm s^{-1} (Neirynck et al., 2007) and 2–3 cm s^{-1} on average (Duyzer, 1994; Zimmerman et al., 2006). Fig. 8 presents the deposition velocities calculated by CAMx over the entire 4-km modeling domain. In Fig. 8 the black dotted line shows the maximum velocities, the solid black line shows the average velocities, and the red line shows the velocities at RMNP alone. The maximum deposition velocities estimated by CAMx varied between 10 and 50 cm s^{-1}, while at RMNP deposition velocities ranged

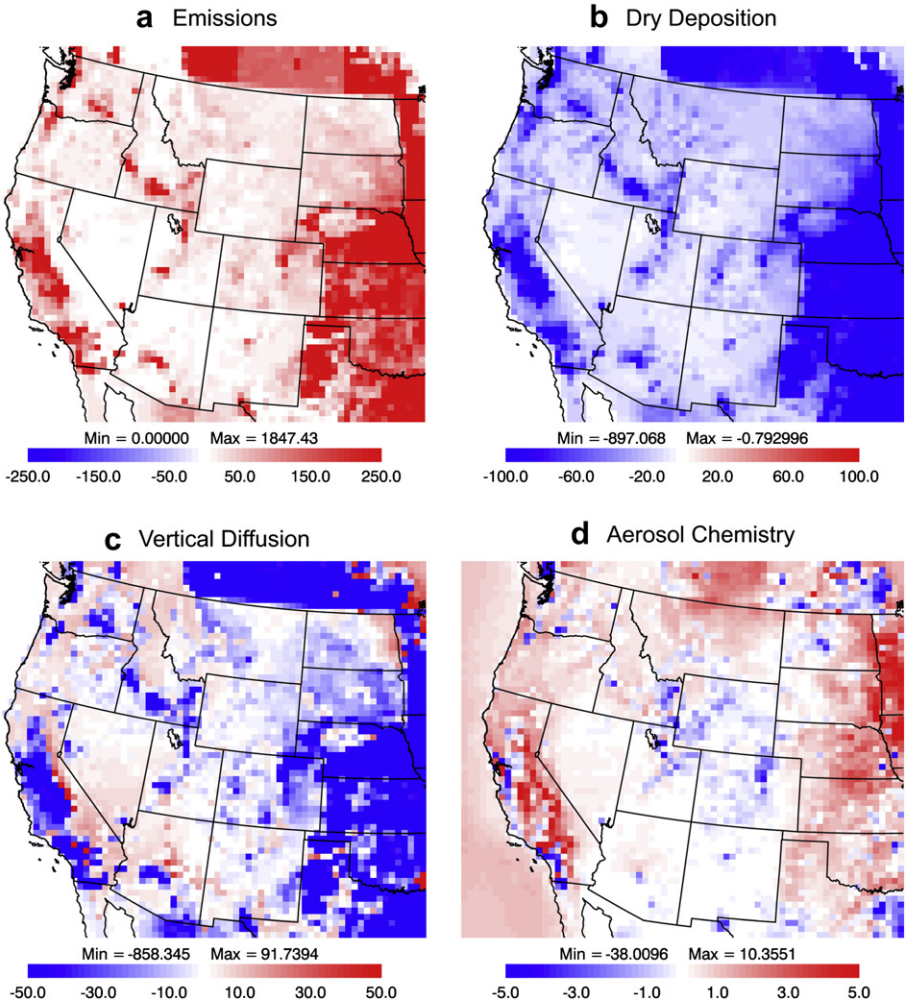

Fig. 6. Spatial distribution of different Integrated Processes Rates affecting ammonia concentrations in the 36-km domain centered in the western United States.

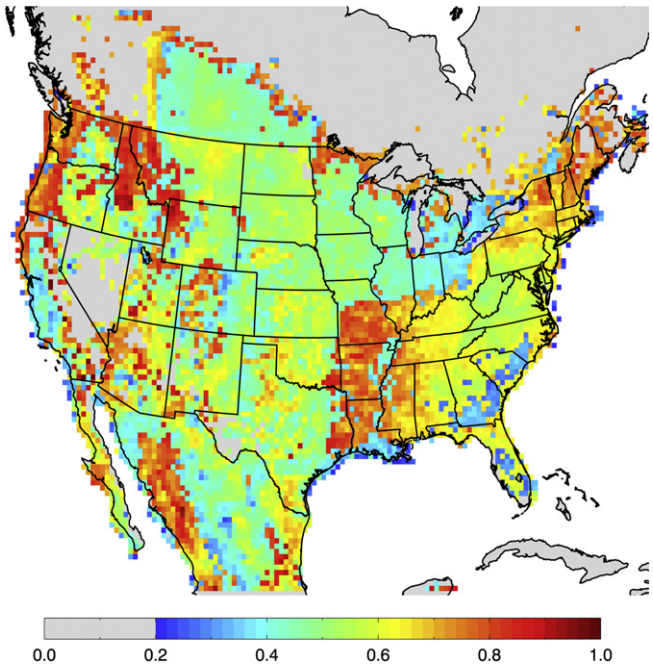

Fig. 7. Fraction of the mass loss through dry deposition relative to the total available mass (the summation of any existing mass plus the net positive flux due to the all the processes) in each cell of the 36-km domain.

between 0.5 and 10 cm s^{-1}, with an average of 5 cm s^{-1}. Fig. 8 illustrates that NH_3 deposition velocities in the model were at least a factor of 2 and in some instances a factor of 10 too high compared with values found in the literature, corroborating the PA results that ammonia removal in the model by dry deposition was certainly overestimated for the RoMANS simulations.

CAMx determines a deposition velocity for each landuse type in a given cell and then linearly combines them according to the fractional distribution of land use. The deposition flux is then used as the lower boundary condition in the vertical diffusion algorithm. The model uses the Wesely (1989) dry deposition resistance model for gases (ENVIRON, 2005). The deposition velocity v_d is calculated from three primary resistances r in series:

$$v_d = \frac{1}{r_a + r_b + r_s} \quad (2)$$

The aerodynamic resistance r_a represents bulk transport through the lowest model layer by turbulent diffusion. The quasi-laminar sublayer resistance r_b represents molecular diffusion through the thin layer or air directly in contact with the particular surface to which material is being deposited. Finally, over land the surface resistance r_s is further expressed as several more serial and parallel resistances that depend upon the physical and chemical properties of the surface in question, such as the pathway into the stomatal and mesophyllic portions of active plants.

Further inspection of the model deposition velocity parameterization in this study indicated that CAMx sets the surface resistance for NH_3 to zero through the chemistry parameters file. This CAMx setup essentially assumes that given the strong rates of uptake by biota and other surfaces, the surface resistance of NH_3 is set to zero, just as that of strong acids like nitric and hydrochloric acid. Neglecting the surface resistance term could be playing an important role in the observed overestimation of NH_3 deposition velocities. Zhang et al. (2003) presented a revised parameterization for gaseous dry deposition in air quality models and discussed detailed revisions to r_s, noting that the uncertainties in r_a and r_b from the different models are small. Zhang's parameterization predicted maximum dry deposition velocities for NH_3 between 0.8 and 4 cm s^{-1}, depending on land use category and dry or wet canopies. These values are in better agreement with those reported in the literature. Future versions of CAMx will provide the option to choose between Wesely and Zhang's parameterizations (Ralph Morris personal communication); however, at the time of this study Zhang's deposition scheme was not available.

Nonetheless, it was still possible to evaluate the effect of NH_3 deposition velocities on model simulations by using the current dry deposition parameterization. A number of sensitivity simulations were made by applying simple uniform scaling factors (without spatial or temporal variation) to the current NH_3 deposition velocities. An additional sensitivity simulation was performed by replacing the NH_3 dry deposition velocity with that of sulfur dioxide. This case was considered given the recent work done by the U.S. Environmental Protection Agency (EPA) Atmospheric Modeling Division with the Community Multiscale Air Quality (CMAQ) model, which showed that ammonia deposition velocities

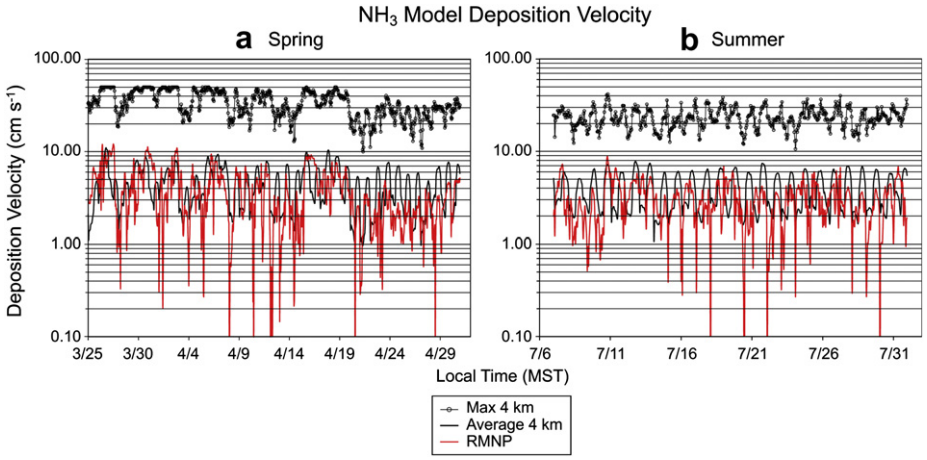

Fig. 8. Model estimated deposition velocities for the 4-km domain (in black) and at Rocky Mountain National Park (RMNP) (in red) for both spring and summer. The line with circles shows the domain-wide maximum values, while the solid line shows the domain-wide average. For this figure, the domain-wide maximum values of sulfur dioxide deposition velocities (vdso2) range between 0.5 and 2 cm s^{-1} for both spring and summer (For interpretation of the references to color in this figure legend, the reader is referred to the web version of this article.).

should be similar to the values for sulfur dioxide deposition or even lower over some land use surface types (U.S. EPA, 2008). Table 3 shows the estimated model biases across the RoMANS sites during spring for the different sensitivity simulations.

While none of the sensitivity simulations showed a significant improvement in the model performance, in at least one case, the bias was reduced on average, although the precision was no better than the base case simulation. The simulation with the original deposition velocities decreased by a factor of 2 ($v_d/2$) still showed a systematic negative bias but was smaller in magnitude, although the correlation with observations was still very poor. Setting the deposition velocities to a domain-wide value of 5 cm s^{-1} led to even larger systematic negative biases than the base case. Finally, replacing the ammonia deposition velocities with those of sulfur dioxide in general caused the model to overestimate NH_3 observations. A more detailed time series comparison between these sensitivity cases and observations at RMNP is shown in Fig. 9. The main point illustrated by this figure is that changing the original deposition velocities with a simple multiplicative scaling factor did not improve the timing of episodes in any of the sensitivity simulations. In particular, none of the cases was able to reproduce the observed episode during April 23.

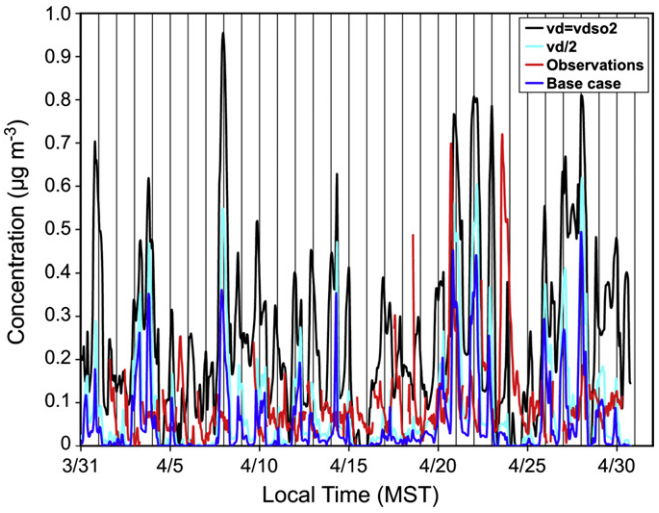

Fig. 9. Time series comparison between sensitivity simulation cases and observations at Rocky Mountain National Park. Sensitivity case vd/2 refers to original NH_3 deposition velocities divided by a factor of 2, while vd = vdso2 refers to the original NH_3 deposition velocities replaced by those of SO_2.

6. Discussion

The model performance evaluation presented here showed that in the Rocky Mountain region, and during the period when the RoMANS field measurements took place, CAMx was not able to properly reproduce within a reasonable uncertainty the observed NH_3 concentrations at any of the available observational sites. While the model performance for other species varied by season and site, ranging from good to poor, the performance for these species was comparable to other model evaluations for this region, e.g., regional haze modeling performed by the WRAP-RMC (Tonnesen et al., 2006). The poor performance of the model for NH_3 and total reduced nitrogen restricted its use to address important questions related to the source apportionment of different emission source regions and sectors, the primary objective of the modeling component of RoMANS. These deficiencies in simulating reduced nitrogen might not be limited to CAMx and could also occur with other regional models. Model intercomparison studies focusing on NH_3 performance should be conducted to investigate this issue.

In this study, the CAMx IPR analysis tool was used to investigate the numerical processes underlying the model predictions to better understand the causes of the poor model performance. IPR is a powerful diagnostic tool that is beginning to be more widely used by the air quality modeling community. The IPR analysis showed that dry deposition was the most important NH_3 removal mechanism, while aerosol chemistry processes played a small role in the simulated concentrations. An examination of the deposition velocities estimated by CAMx shows they could be overestimated by up to a factor of 10 relative to values reported in the literature. Closer inspection of the deposition velocity parameterization revealed that the surface resistance term was neglected. This needs to be addressed in future work, possibly through the use of a different dry deposition parameterization implemented in a more recent version of CAMx. This study also presented a subsequent suite of sensitivity simulations that modified the values of the dry deposition velocity, and although not exhaustive, led to the conclusion that even when the dry deposition values were "fixed" or altered to reduce their influence, the model was still unable to replicate the observed time series; i.e., it addressed the average bias, but it did not improve the precision.

Since NH_3 is a primary, emitted species that does not react in the gas phase, and because the IPR analysis showed that the aerosol chemistry processes appeared to play a small role in the simulated concentrations, it is also possible that the NH_3 emissions inventory might be underestimated, or that the location and timing of NH_3 fluxes were misrepresented, leading to the negative biases evident in the model performance evaluation. Furthermore, a recent study that employed satellite observations found that ammonia emissions in the mid-latitudes could be significantly underestimated (Clarisse et al., 2009). Clearly, there are significant uncertainties within the existing ammonia emission inventories, and addressing these by incorporating current ammonia emission flux research (e.g., Baum and Ham, 2009) would substantially increase our confidence in the model predictions.

Table 3
Mean Fractional Bias estimates across various RoMANS sites during spring 2006 for different simulations with varying dry deposition velocities of NH_3. The names and locations of sites correspond to those presented in Fig. 2.

	Spring NH_3 Sensitivity Simulations MFB (%)								
	Site 1[a]	Site 2	Site 3	Site 5	Site 6	Site 7	Site 8	Site 9	Site 10
Base case (V_d[b])	−171	−41	−62	−107	−125	−113	−160	−118	−86
$V_d/2$[c]	−159	−5	−9	−60	−90	−83	−142	−76	−49
$V_d = V_{SO2}$[d]	−137	93	115	62	19	−38	−119	−13	−6
V_d = 5 cm s^{-1} [e]	−193	−111	−106	−139	−165	−168	−190	−175	−160

[a] Refer to legend on Fig. 2 for names and locations that correspond to site numbers.
[b] NH_3 original deposition velocities.
[c] Original deposition velocities divided by factor of 2.
[d] Original deposition velocities replaced by those of SO_2.
[e] Original deposition velocities changed by 5 cm s^{-1} domain-wide.

As a result of RoMANS, the National Park Service decided to look at year-long trends of NH_3 ambient concentrations and deposition at the core site. The measurements were made from November 2008 to November 2009, and it is expected that a modeling effort will be performed for this period. Future work will involve a year-long CAMx simulation for this period. That simulation will use an updated emissions inventory for NH_3 that will be revisited and likely improved with new information pertinent for Colorado; also the new modeling effort will include Zhang's dry deposition parameterization. Many aspects presented in this study will be revisited and implemented; for instance, a limitation of the current study is that the process analysis work does not consider different spatial scales. It is not surprising that when limiting the IPR aggregation to the first layer, vertical transport processes dominate. CAMx provides the ability to aggregate process rates vertically to the top of the simulated planetary boundary layer (PBL). By doing this it should reduce the dominance of vertical transport and permit an evaluation of processes within the well-mixed volume below the PBL. Furthermore, expanding the horizontal aggregation would also minimize horizontal transport and better capture the processes upwind of the core site. With these changes a more spatially balanced comparison of all processes can be made.

Acknowledgments

We are grateful to the people responsible for some of the key datasets used in this study. Christian Carrico was responsible for continuous gas measurements at the core site. Taehyoung Lee (spring) and Amy Sullivan (summer) were responsible for the continuous PILS NH_4^+ concentrations. Data from the other sites are the result of efforts by Florian Schwandner, Katie Beem, Suresh Raja, Courtney Taylor, Derek Day, and Gavin McMeeking. Dr Sonia Kreidenweis was co-Principal Investigator of the field measurement efforts. The assumptions, findings, conclusions, judgments, and views presented herein are those of the authors and should not be interpreted as necessarily representing the National Park Service policies.

Appendix. Supplementary data

Supplementary data associated with this article can be found in the online version, at doi:10.1016/j.atmosenv.2010.09.011.

References

Andersen, H.V., Hovmand, M.F., Hummelshoj, P., Jensen, N.O., 1993. Measurements of ammonia flux to a spruce stand in Denmark. Atmospheric Environment Part A-General Topics 27, 189–202.

Andersen, H.V., Hovmand, M.F., 1995. Ammonia and nitric acid dry deposition and throughfall. Water and Soil Pollution 85, 2211–2216.

Andersen, H.V., Hovmand, M.F., 1999. Review of dry deposition measurements of ammonia and nitric acid to forest. Forest Ecology and Management 114, 5–18.

Andersen, H.V., Hovmand, M.F., Hummelshoj, P., Jensen, N.O., 1999. Measurements of ammonia concentrations, fluxes, and dry deposition velocities to a spruce forest 1991–1995. Atmospheric Environment 33, 1367–1383.

Baum, K.A., Ham, J.M., 2009. Adaptation of a speciation sampling cartridge for measuring ammonia flux from cattle feedlots using relaxed eddy accumulation. Atmospheric Environment 43, 1753–1759.

Baker, K., Scheff, P., 2007. Photochemical model performance for PM2.5 sulfate, nitrate, ammonium, and precursor species SO2, HNO3, and NH3 at background monitor locations in the central and eastern United States. Atmospheric Environment 41, 6185–6195.

Barna, M.G., Gebhart, K.A., Schichtel, B.A., Malm, W.C., 2006. Modeling regional sulfate during the BRAVO study: Part 1. Base emissions simulation and performance evaluation. Atmospheric Environment 40, 2436–2448. doi:10.1016/j.atmosenv.2005.12.040.

Baron, J.S., Rueth, H.M., Wolfe, A.M., Nydick, K.R., Allstott, E.J., Minear, J.T., Moraska, B., 2000. Ecosystem responses to nitrogen deposition in the Colorado Front Range. Ecosystems 3, 352–368.

Baron, J.S., 2006. Hindcasting nitrogen deposition to determine an ecological critical load. Ecological Applications 16 (2), 433–439.

Beem, K.B., Raja, S., Schwandner, F.M., Taylor, C., Lee, T., Sullivan, A.P., Carrico, C.M., McMeeking, G.R., Day, D., Levin, E., Hand, J., Kreidenweis, S.M., Schichtel, B., Malm, W.C., Collett, J.L., Mar 2010. Deposition of reactive nitrogen during the Rocky Mountain Airborne Nitrogen and Sulfur (RoMANS) study. Environmental Pollution 158 (3), 862–872.

Boylan, J.W., Russell, A.G., 2006. PM and light extinction model performance metrics, goals, and criteria for three-dimensional air quality models. Atmospheric Environment 40, 4946–4959.

Clarisse, Lieven, Clerbaux, Cathy, Dentener, Frank, Hurtmans, Daniel, Coheur, Pierre-François, 2009. Global ammonia distribution derived from infrared satellite observations. Nature Geoscience 2, 479–483.

DeBell, L.J., Gebhart, K.A., Hand, J.L., Malm, W.C., Pitchford, M.L., Schichtel, B.A., White, W.H., 2006. Spatial and seasonal patterns and temporal variability of haze and its constituents in the United States Report IV. Available at. http://vista.cira.colostate.edu/improve/Publications/Reports/2006/PDF/IMPROVE_Report_IV.pdf.

Duyzer, J.H., 1994. Dry deposition of ammonia and ammonium aerosols over heathland. Journal of Geophysical Research-Atmospheres 99, 18757–18763.

ENVIRON, 2005. CAMx v.4.20 User's Guide. ENVIRON International Corporation, Novato, CA.

Galloway, J.N., Aber, J.D., Erisman, J.W., Seitzinger, S.P., Howarth, R.W., Cowling, E.B., Cosby, B.J., Apr., 2003. The nitrogen cascade. BioScience 53 (4), 341–356.

Grell, G.A., Dudhia, J., Stauffer, D.R. A description of the fifth generation Penn State/NCAR Mesoscale Model (MM5). NCAR Technical Note (TN-398-STR), NCAR, Boulder, CO, 1994.

Harrison, R.M., Allen, A.G., 1991. Scavenging ratios and deposition of sulfur, nitrogen, and chlorine species in eastern England. Atmospheric Environment Part A-General Topics 25, 1719–1723.

Henderson, B., et al. The influence of model resolution on ozone in industrial plumes. Journal of Air & Waste Management, in press.

Houyoux, M., Vukovich, J., Brandmeyer, J.E., 2002. Sparse Matrix Operator Kernel Emissions Modeling System-SMOKE User Manual; MCNC-2002. Environmental Modeling Center, Research Triangle Park, NC.

IE, 2006. SMOKE version 2.2 Users Manual. Carolina Environmental Program, Chapel Hill, NC. http://www.ie.unc.edu/cempd/products/smoke/version2.2/html/.

Jeffries, H.E., Tonnesen, S., 1994. A comparison of two photochemical reaction mechanisms using a mass balance and process analysis. Atmospheric Environment 28 (18), 2991–3003.

Jiménez, P., Jorba, O., Parra, R., Baldasano, J.M., 2006. Evaluation of MM5-EMICAT2000-CMAQ performance and sensitivity in complex terrain: high-resolution application to the northeastern Iberian Peninsula. Atmospheric Environment 40, 5056–5072. doi:10.1016/j.atmosenv.2005.12.060.

Kimura, Y., et al., 2008. Application of a Lagrangian process analysis tool to characterize ozone formation in Southeast Texas. Atmospheric Environment 42 (23), 5743–5759.

Korb, J.E., Ranker, T.A., 2001. Changes in stand composition and structure between 1981 and 1996 in four Front Range plant communities in Colorado. Plant Ecology 157, 1–11.

Levin, E.J.T., Kreidenweis, S.M., McMeeking, G.R., Carrico, C.M., Collett Jr., J.L., Malm, W.C., April 2009. Aerosol physical, chemical and optical properties during the Rocky Mountain Airborne Nitrogen and Sulfur study. Atmospheric Environment 43 (11), 1932–1939. ISBN 1352-2310. doi:10.1016/j.atmosenv.2008.12.042.

Morris, R.E., Yarwood, G., Emery, C., Koo, B., 2004. Development and application of the CAMx regional one-atmosphere model to treat ozone, particulate matter, visibility, air toxics, and mercury. Presented at the Air & Waste Management Association's 97th Annual Conference and Exhibition, Indianapolis, June.

Morris, Ralph E., Koo, Bonyoung, Guenther, Alex, Yarwood, Greg, McNally, Dennis, Tesche, T.W., Tonnesen, Gail, Boylan, James, Brewer, Patricia, August 2006. Model sensitivity evaluation for organic carbon using two multi-pollutant air quality models that simulate regional haze in the southeastern United States. Atmospheric Environment 40 (26), 4960–4972. ISBN 1352-2310. doi:10.1016/j.atmosenv.2005.09.088. Special issue on Model Evaluation: Evaluation of Urban and Regional Eulerian Air Quality Models.

Malm, W.C., Sisler, J.F., Huffman, D., Eldred, R.A., Cahill, T.A., 1994. Spatial and seasonal trends in particle concentration and optical extinction in the United States. Journal of Geophysical Research 99, 1347–1370.

Malm, W.C., Collett, J.L., Barna, M.G., Beem, K., Carrico, C.M., Gebhart, K.A., Hand, J.L., Levin, E., Rodriguez, M.A., Schichtel, B.A., Schwandner, F., 2009. Rocky Mountain Atmospheric Nitrogen and Sulfur Study Report. National Park Service/Colorado State University. ISSN 0737-5352-84.

Mansell, G., 2005. Final Report Volume I – An Improved Ammonia Inventory for the WRAP Domain, Prepared for the Western Governors' Association. ENVIRON International Corp., Novato, CA. http://pah.cert.ucr.edu/aqm/308/ppt_files/emissions/nh3/Volume_I_FinalReport.3-07.pdf.

Morris, R., et al., 2007. Technical Support Document for VISTAS Emissions and Air Quality Modeling to Support Regional Haze SIP Implementation Plans. Prepared for VISTAS by ENVIRON, et al., Novato, CA. http://www.carallc.net/pdfs/9%20%20VISTAS%20Phase%20II%20Final%20Report.pdf.

Neirynck, J., Kowalski, A.S., Carrara, A., Genouw, G., Berghmans, P., Ceulemans, R., 2007. Fluxes of oxidized and reduced nitrogen above a mixed coniferous forest exposed to various nitrogen emission sources. Environmental Pollution 149 (1), 31–43.

Nemitz, E., Sutton, M.A., Wyers, G.P., Jongejan, P.A.C., 2004. Gas-particle interactions above a Dutch heathland: I. Surface exchange fluxes of NH3, SO2, HNO3, and HCl. Atmospheric Chemistry and Physics 4, 989–1005.

Nenes, A., Pandis, S.N., Pilinis, C., 1999. Continued development and testing of a new thermodynamic aerosol module for urban and regional air quality models. Atmospheric Environment 33, 1553–1560.

Nydick, K.R., Lafrancois, B.M., Baron, J.S., Johnson, B.M., 2004. Nitrogen regulation of algal biomass, productivity, and composition in shallow mountain lakes, Snowy Range, Wyoming, USA. Canadian Journal of Fisheries and Aquatic Sciences 61, 1256–1268.

Odman, M.T., Ingram, C., 1996. Multiscale Air Quality Simulation Platform (MAQSiP): Source Code Documentation and Validation. Technical Report ENV-96TR002. Research Triangle Park, NC, MCNC (Microelectronics Center of North Carolina).

Pechan, 2003. WRAP Interim 2002 Point and Area Source Emission Estimates: Technical Memorandum. Prepared for Western Governors' Association by E.H. Pechan and Associates, Springfield, VA. http://www.wrapair.org/forums/ef/inventories/2002/Interim_2002_Point_and_Area_EI_Technical_Memorandum.pdf.

Pun, B.K., Seigneur, Christian, Vijayaraghavan, Krish, Wu, Shiang-Yuh, Chen, Shu-Yun, Knipping, Eladio M., Kumar, Naresh, 2006. Modeling regional haze in the BRAVO study using CMAQ-MADRID: 1. Model evaluation. Journal of Geophysical Research-Atmospheres 111, D06302. doi:10.1029/2004JD005608.

Seigneur, C., Pun, B., Pai, P., Louis, J.F., Solomon, P., Emery, C., Morris, R., Zahniser, M., Worsnop, D., Koutrakis, P., White, W., Tombach, I., 2000. Guidance for the performance evaluation of three-dimensional air quality modeling systems for particulate matter and visibility. Journal of the Air & Waste Management Association 50 (4), 588–599.

Song, J., et al., 2008. Comparisons of modeled and observed isoprene concentrations in southeast Texas. Atmospheric Environment 42 (8), 1922–1940.

Tesche, T.W., Morris, R., Tonnesen, G., McNally, D., Boylan, J., Brewer, P., 2006. CMAQ/CAMx annual 2002 performance evaluation over the eastern US. Atmospheric Environment 40, 4906–4919. doi:10.1016/j.atmosenv.2005.08.046.

Tonnesen, G., Wang, Z., Omary, M., Chien, C.-J., Wang, Y., Morris, R., Kemball-Cook, S., Jia, Y., Lau, S., Koo, B., Adelman, Z., Holland, A.C., Wallace, J., 2006. Final Report for the Western Regional Air Partnership (WRAP) 2002 Visibility Model Performance Evaluation. Western Governors' Association. WGA Contract Number 30203.

U.S. EPA. Integrated Science Assessment (ISA) for Oxides of Nitrogen and Sulfur Ecological Criteria (Final Report). U.S. Environmental Protection Agency, Washington, DC, EPA/600/R-08/082F, 2008.

Vizuete, W.V., et al., 2008. Modeling ozone formation from industrial emission events in Houston, Texas. Atmospheric Environment 42 (33), 7641–7650.

Wang, Z., Langstaff, J.E., Jeffries, H.E., 1995. The Application of the Integrated Process Analysis Rate Analysis Method for Investigation of Urban Airshed Model (UAM) Sensitivity to Speciation in VOC Emissions Data. Air & Waste Management Association annual meeting, San Antonio, TX.

Wesely, M.L., 1989. Parameterization of surface resistance to gaseous dry deposition in regional-scale numerical models. Atmospheric Environment 23, 1293–1304.

Whitten, G., Deuel, H.P., Burton, C.S., Haney, J.L., 1996. Memorandum to OTAG participants: overview of the implementation of an updated isoprene chemistry mechanism in CB4/UAM-V.

Yarwood, G., Stoeckenius, T.E., Heiken, J.G., Dunker, A.M., 2003. Modeling weekday/weekend ozone differences in the Los Angeles region for 1997. Journal of the Air & Waste Management Association 53, 864.

Zhang, L., Brook, J.R., Vet, R., 2003. A revised parameterization for gaseous dry deposition in air-quality models. Atmospheric Chemistry and Physics 3, 2067–2082.

Zhang, Y., Vijayaraghavan, K., Seigneur, C., 2006. Evaluation of three probing techniques in a three-dimensional air quality model. Journal of Geophysical Research-Atmospheres 110, D02305. doi:10.1029/2004JD005248.

Zimmerling, R., Dammgen, U., Grunhage, L., Haenel, H.D., Kusters, A., Max, W., Jager, H.J., 1997. The classifying ratiometric method for the continuous determination of atmospheric flux densities of reactive N- and S- species with denuder filter systems. Journal of Applied Botany-Angewandte Botanik 71, 38–49.

Zimmerman, F., Plessow, K., Queck, R., Bernofer, C., Matschullat, J., 2006. Atmospheric N and S-fluxes to a spruce forest – comparison of inferential modeling and the throughfall method. Atmospheric Environment 40, 4782–4796.